Landes Bioscience

www.landesbioscience.com

Supplemental Material to:

Sue Haupt, Catherine Mitchell, Vincent Corneille, Jake Shortt, Stephen Fox, Pier Paolo Pandolfi, Mireia Castillo-Martin, Dennis M. Bonal, Carlos Cordon-Carlo, Guillermina Lozano and Ygal Haupt

Loss of PML cooperates with mutant p53 to drive more aggressive cancers in a gender-dependent manner

2013; 12(11)

http://dx.doi.org/10.4161/cc.24805

http://www.landesbioscience.com/journals/cc/article/24805

Supplementary Figure 1

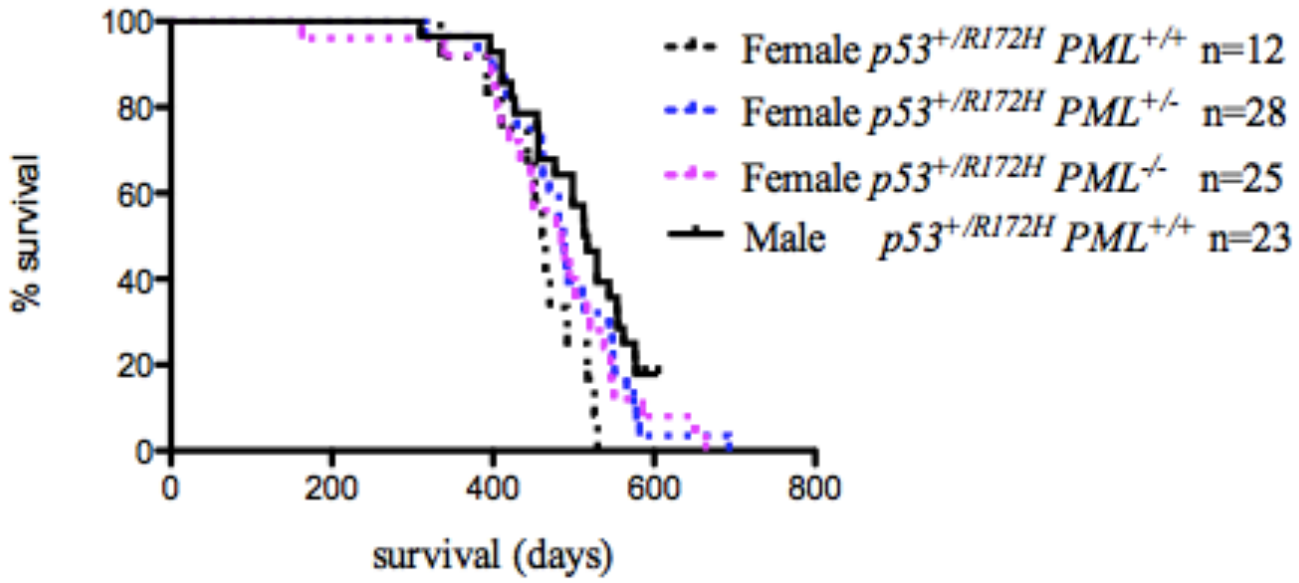

	Female *p53*$^{+/R172H}$ *PML*$^{+/+}$	**Female *p53*$^{+/R172H}$ *PML*$^{+/-}$**	**Female *p53*$^{+/R172H}$ *PML*$^{-/-}$**	**Male *p53*$^{+/R172H}$ *PML*$^{+/+}$**
Median survival	463d*	488d*	485d*	515d*
No. Mice	12	28	25	23

*Curves No Sig Diff by Mantel Cox Test p= 0.0609

Supplementary Figure 2

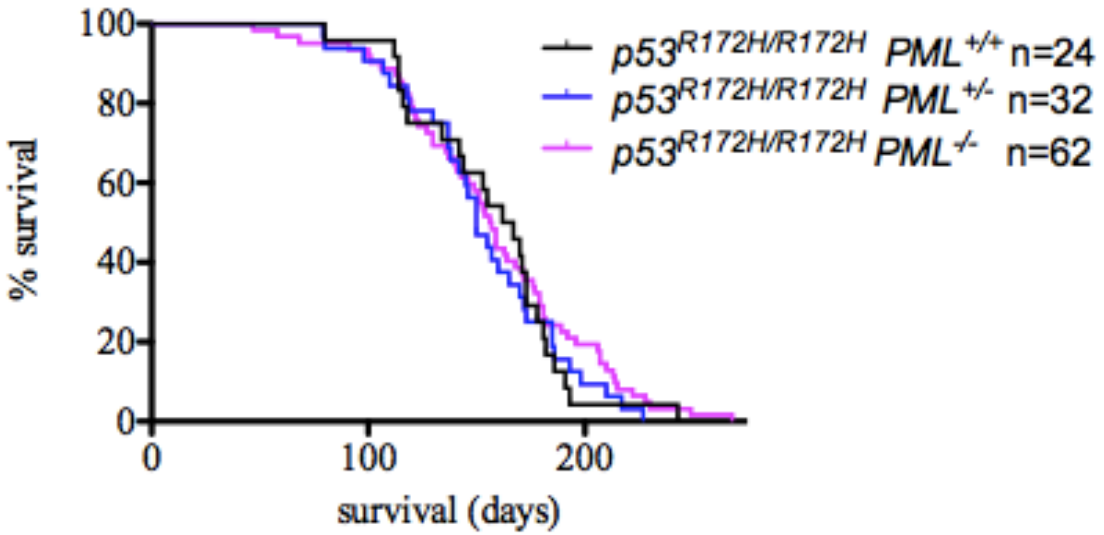

Males	***p53*$^{R172H/R172H}$ *PML* $^{+/+}$**	***p53*$^{R172H/R172H}$ *PML* $^{+/-}$**	***p53*$^{R172H/R172H}$ *PML*$^{-/-}$**
Median survival	164.5d	150d	156.5d
No. Mice	24	32	62

*Curves No Sig Diff by Mantel Cox Test p= 0.6136

Supplementary Figure 3

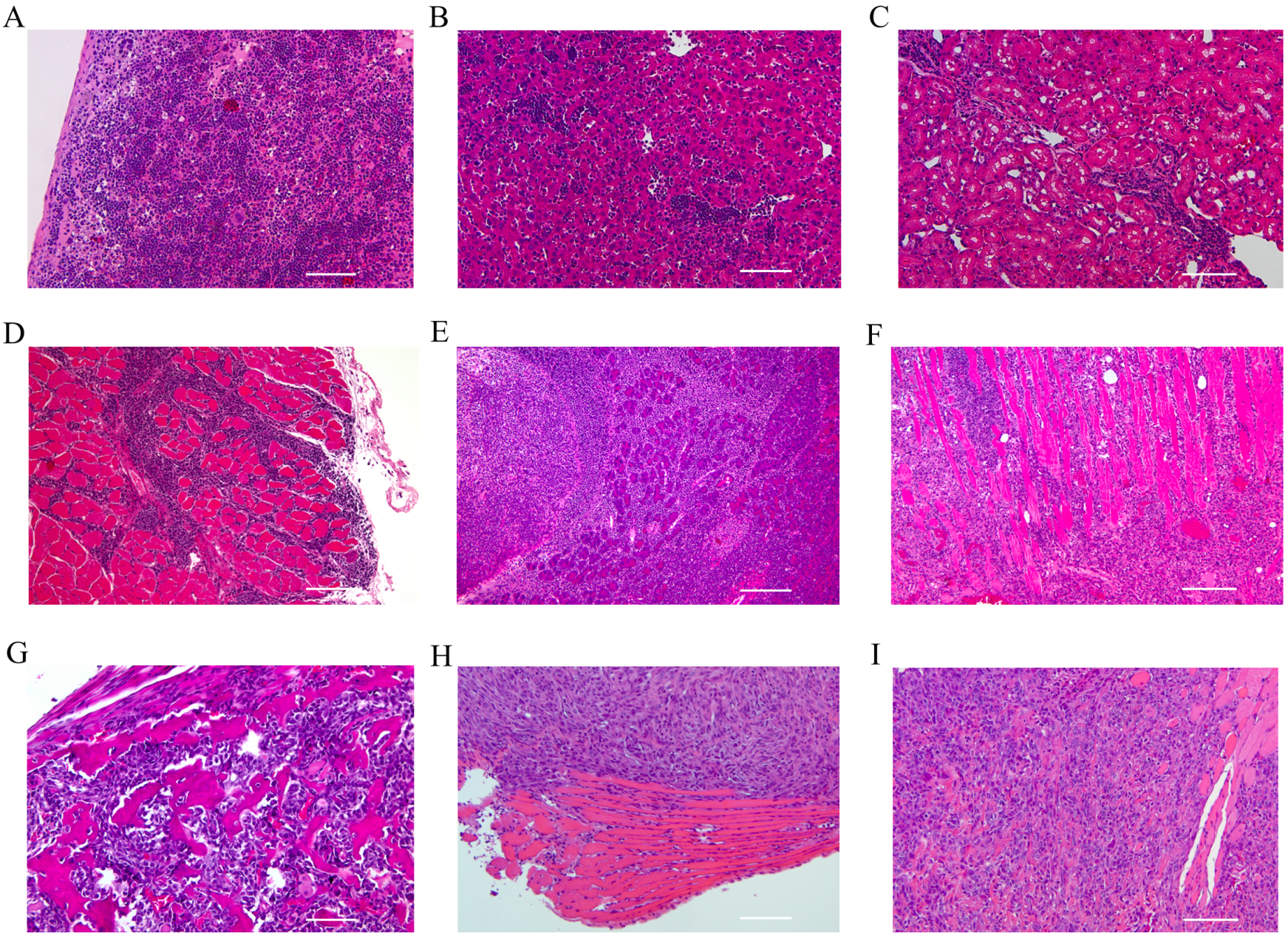

Supplementary Figure 4

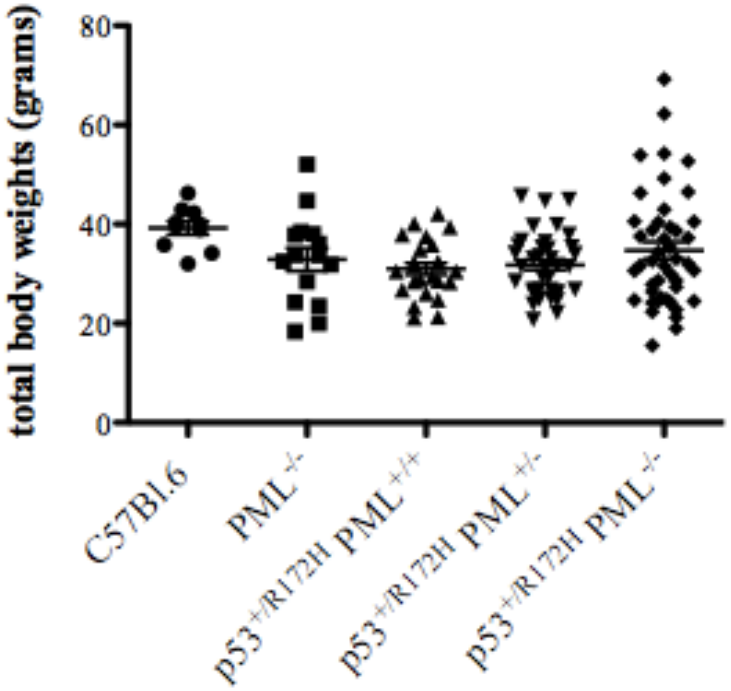

	C57BL.6	*PML*$^{-/-}$	*p53*$^{+/R172H}$ *PML*$^{+/+}$	*p53*$^{+/R172H}$ *PML*$^{+/-}$	*p53*$^{+/R172H}$ *PML*$^{-/-}$
***mean body weight**	39.24	32.90	**31.00**	**31.79**	34.70
***p-value relative to C57BL.6**		ns 0.0521	s 0.0003	s 0.0011	ns 0.2296
no. mice	10	15	24	37	45

*significance (s) or no significance (ns) was determined using the unpaired t-test; $p<0.05$, where all values were compared to C57Bl.6

Supplementary Figure 5

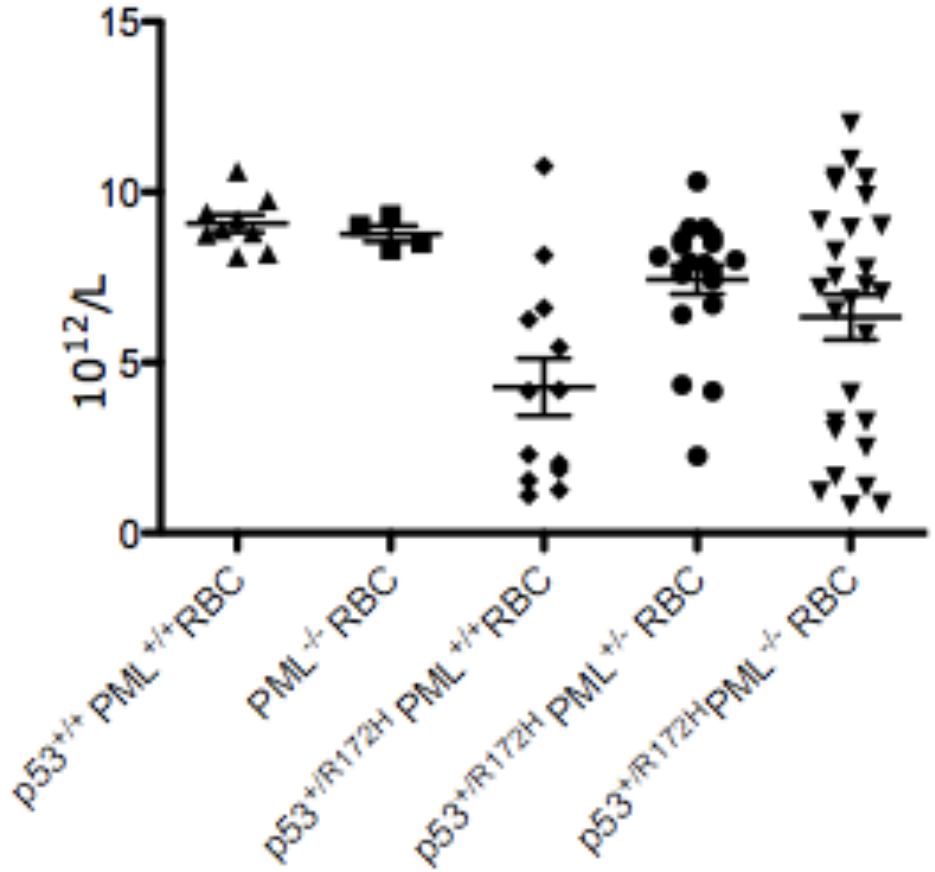

Supplementary Figure 6

lymphomas

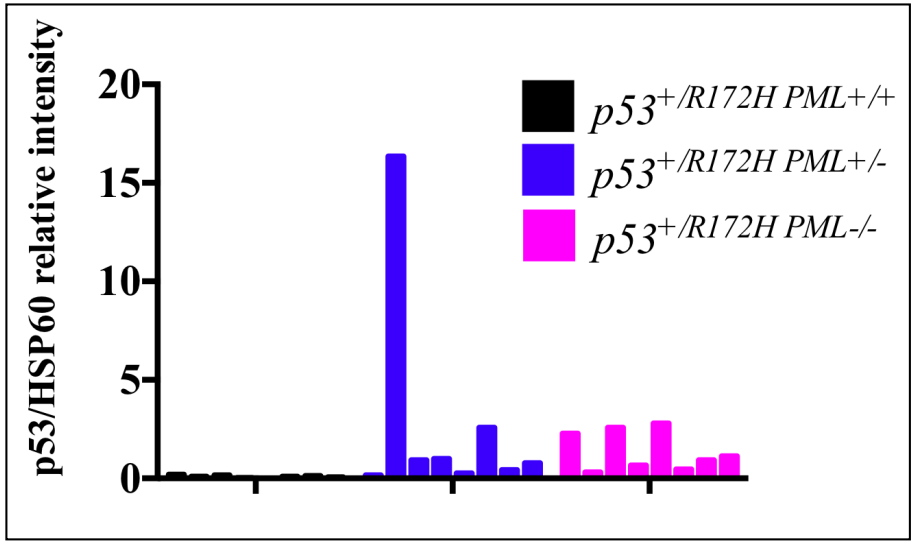

sarcomas

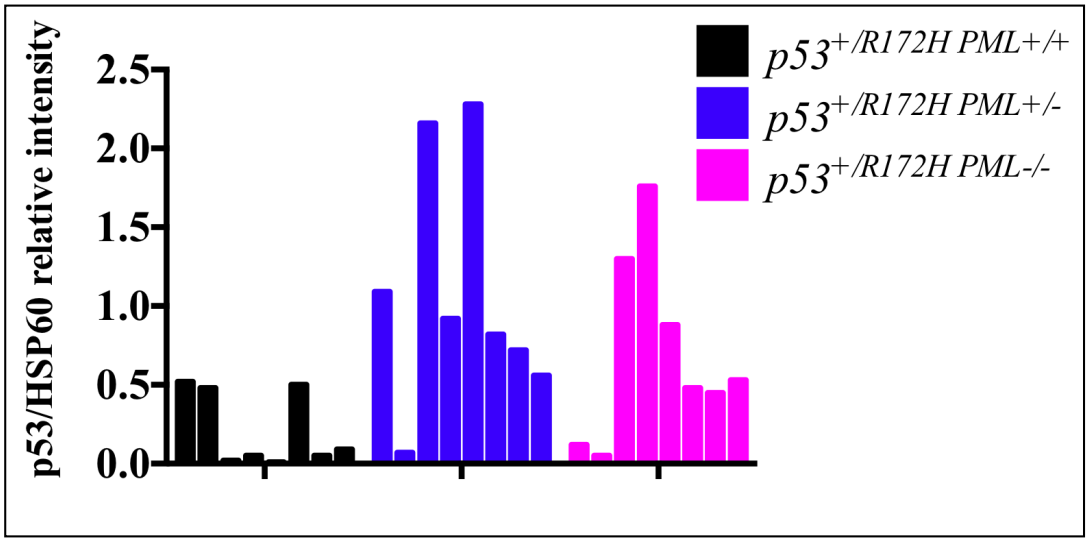

Supplementary Figure 7

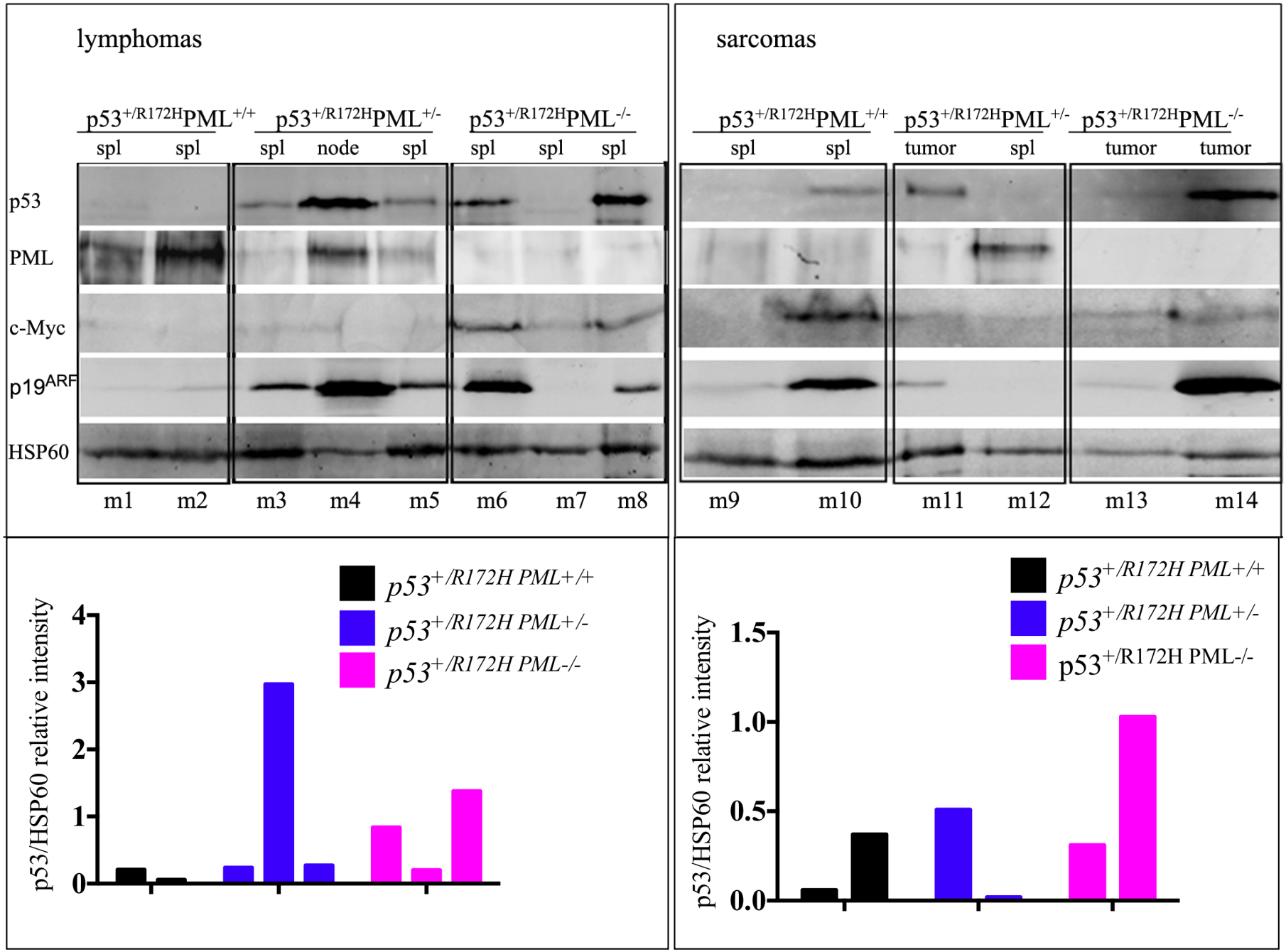

Supplementary Table 1

Female survival is severely reduced in *p53*$^{R172H/R172H}$ mice and this is not altered by PML loss

	***p53*$^{+/+}$ *PML*$^{+/+}$**	***p53*$^{+/+}$ *PML*$^{+/-}$**	***p53*$^{+/+}$ *PML*$^{-/-}$**
XX	27 (47%)	61 (42%)	139 (46%)
XY	30 (53%)	83 (58%)	163 (54%)
SUM	57	144	302

	***p53*$^{+/R172H}$ *PML*$^{+/+}$**	***p53*$^{+/R172H}$ *PML*$^{+/-}$**	***p53*$^{+/R172H}$ *PML*$^{-/-}$**
XX	173 (46%)	81 (42%)	102 (43%)
XY	206 (54%)	112 (54%)	135 (57%)
SUM	80	193	237

	***p53*$^{R172H/R172H}$ *PML*$^{+/+}$**	***p53*$^{R172H/R172H}$ *PML*$^{+/-}$**	***p53*$^{R172H/R172H}$ *PML*$^{-/-}$**
XX	9 (11%)	6 (12%)	7 (9%)
XY	71 (89%)	45 (88%)	74 (91%)
SUM	80	51	81

Supplementary Table 2A

Splenomegaly is evident in *p53*$^{+/R172H}$ mice

	C57BL.6	***PML*$^{-/-}$**	***p53*$^{+/R172H}$ *PML*$^{+/+}$**	***p53*$^{+/R172H}$ *PML*$^{+/-}$**	***p53*$^{+/R172H}$ *PML*$^{-/-}$**
***Mean spleen weight (% of body weight)**	0.2107	0.4089	**4.516**	1.858	1.362
Fold change relative to control C57BL.6	1	2	**21**	9	6.5
***p-value relative to C57BL.6**		s 0.0031	s 0.0003	ns 0.0765	s 0.0241
no. mice	10	16	22	37	45

Supplementary Table 2B

Hepatomegaly is evident in *p53*$^{+/R172H}$ mice

	C57BL.6	***PML*$^{-/-}$**	***p53*$^{+/R172H}$ *PML*$^{+/+}$**	***p53*$^{+/R172H}$ *PML*$^{+/-}$**	***p53*$^{+/R172H}$ *PML*$^{-/-}$**
***mean liver weight (% of body weight)**	4.791	5.270	**11.07**	7.117	6.188
fold change relative to control C57BL.6	1	1	**2**	1.5	1
***p-value relative to C57BL.6**		ns 0.3146	s 0.0131	ns 0.2437	ns 0.2275
no. mice	6	14	23	36	45

*significance (s) or no significance (ns) was determined using the unpaired t-test; $p<0.05$, where all values were compared to C57Bl.6

Supplementary Table 3

A sub-population of Leiomyosarcomas exhibited coincident PML depletion and p53 positivity

Tumor Type	**PML depletion % (cases/total)**	**p53 positivity % (cases/total)**
well differentiated liposarcoma	50 (3/6)	0 (0/6)
myxoid liposarcoma, low grade	0 (0/2)	0 (0/2)
myxoid liposarcoma, high grade	0 (0/5)	0 (0/5)
pleomorphic liposarcoma	100 (2/2)	0 (0/2)
dedifferentiated liposarcoma	13 (1/8)	13 (1/8)
malignant fibrous histiocytoma	20 (2/10)	0 (0/10)
low grade fibromyxoid sarcoma	0 (0/3)	0 (0/3)
leiomyosarcoma	**75 (6/8)**	**25 (2/8)**

Supplementary Figure Legends

S Figure 1. Kaplan-Meir survival curves for female $p53^{+/R172H}$ mice were little effected by *PML* depletion.

S Figure 2. Kaplan-Meir survival curves for $p53^{R172H/R172H}$ mice were not reduced by *PML* depletion.

S Figure 3. $p53^{+/R172H}$ mice presented with EMH in the spleen (A); liver (B) and kidney (C) as demonstrated for $p53^{+/R172H}PML^{+/+}$ mice; and also in smooth muscle (D) as presented for a $p53^{+/R172H}PML^{+/-}$ mouse. Lymphoma (E) and leiomyosarcoma (F) and osteosarcoma (G) were identified as shown for $p53^{+/R172H}PML^{+/-}$ mice; and undifferentiated pleiomorphic sarcoma in skeletal muscle (H) and osteosarcoma (I), as demonstrated for $p53^{+/R172H}PML^{-/-}$ mice. Note: while the pathology is shown for individual genotypes, Table 1 defines prevalence of these manifestations. Tissue sections were stained for hematoxylin and eosin and visualized using a BX-51 microscope (Olympus) fitted with a x25 objective lens and 100μM increments are marked. Pictures were acquired using SPOT Version 4.7 software (Diagnostic Instruments).

S Figure 4. Disease manifestation in $p53^{+/R172H}$ mice. Significant loss of body weight was most pronounced in $p53^{+/R172H}$ mice with PML.

S. Figure 5. Hematological disruption in $p53^{+/R172H}$ mice was evidenced by reduced red blood cell counts in $p53^{+/R172H}$ mice with *PML*.

S. Figure 6. Densitometric analysis of p53 levels normalized to HSP60 for the Western immunoblots in Figure 4: where a range of tissues from $p53^{+/R172H}$ mice ($p53^{+/R175H}$ $PML^{+/+}$; $p53^{+/R175H}$ $PML^{+/-}$; $p53^{+/R175H}$ $PML^{-/-}$) diagnosed with lymphomas (left panel) and sarcomas (right panel) were stained for p53 and HSP60.

S. Figure 7. Western immunoblotting of a range of tissues (spleens (spl.), node, tumor) from $p53^{+/R172H}$ mice (m 1-14) stained for p53, $p19^{ARF}$, c-Myc and HSP60 diagnosed with lymphomas and sarcomas. Lymphomas from genotypes ($p53^{+/R175H}$ $PML^{+/+}$; $p53^{+/R175H}$ $PML^{+/-}$; $p53^{+/R175H}$ $PML^{-/-}$) are shown on a single blot (left panel), and sarcomas (right panel) on a second (with superimposed black boxes to assist visual alignment). Densitometric analysis of p53 levels normalized to HSP60 are displayed directly underneath the corresponding Western immunoblot.